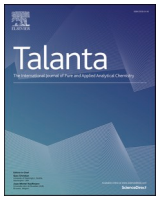
Talanta 294 (2025) 128161



Contents lists available at ScienceDirect

Talanta

journal homepage: www.elsevier.com/locate/talanta



Structure-switchable dsDNA promoter regulates the activity of CRISPR-Cas12a for APE1 detection

Xingrong Li [a,1], Yumei Li [a,1], Cuixiang Wang [a], Jiatong Chai [a], Hongmao Liu [a], Xinli Jiang [a], Yirong Li [a,b,c,d,*]

[a] Department of Laboratory Medicine, Zhongnan Hospital of Wuhan University, Wuhan University, Wuhan, People's Republic of China
[b] Wuhan Research Center for Infectious Diseases and Cancer, Chinese Academy of Medical Sciences, Wuhan, People's Republic of China
[c] Hubei Engineering Center for Infectious Disease Prevention, Control and Treatment, Wuhan, People's Republic of China
[d] Hubei Provincial Clinical Medical Research Center for Molecular Diagnostics, Wuhan, People's Republic of China

ARTICLE INFO

Keywords:
APE1
CRISPR/AsCas12a
Structure-switchable
Site-directed incision
Molecular diagnostics

ABSTRACT

Apurinic/apyrimidinic endonuclease 1 (APE1) has been considered as a promising biomarker since it is associated with numerous human diseases, involving neurodegenerative diseases and cancer. However, current APE1 detection methods mainly rely on immunology-based methods, which are burdened by time-consuming and procedural complexity. To overcome these shortcomings, we have developed an innovative all-in-one technique that simplifies APE1 detection by integrating enzyme-responsive elements structure-switchable dsDNA promoter with CRISPR/AsCas12a methodology, namely EDC. In this work, the structure-switchable dsDNA promoter has been well-designed to trigger the site-directed incision of APE1 and then release the split activator to illumine the CRISPR/AsCas12a catalyst system by coupling it with another truncated activator. Under optimal circumstances, the proposed strategy enables sensitive detection of the target APE1 with a detection limit of 4.8×10^{-5} U/mL and a wide linear range from 5.0×10^{-5} to 1.0×10^{-1} U/mL. Moreover, this strategy could be gratifyingly applied to screen APE1 inhibitors and monitor APE1 in lysates from cell extractions or clinical serum samples. Overall, this study presents a novel approach that utilizes dsDNA promoter as programmable switching components, effectively enhancing CRISPR/Cas12a-based diagnostic platforms and demonstrating the significant potential for clinical translation.

1. Introduction

APE1 (Apurinic/apyrimidinic endonuclease effector factor) is a critical enzyme in the DNA repair process, participating in the DNA damage BER (base excision repair) pathway by carving the dsDNA to put the cleavage locus in the specific sites to facilitate nucleophilic attack within its compact protein active site [1–3]. In addition to DNA repair, APE1, also commonly recognized as redox factor-1, plays a crucial function in the reductive activation of most transcription factors, regulation of gene expression and facilitating cell response to oxidative stress, which is linked to diverse cellular physiological processes such as growth signaling, inflammatory and anti-apoptotic pathways [4]. Evidence has shown that the expression of APE1 in tumor tissues (such as cervical cancer, lung cancer, and primary liver cancer) is significantly different from those in the corresponding normal tissues. Furthermore, some previous research has proven that inhibiting APE1 activity increases the cellular susceptibility to therapeutic agents, indicating a direct correlation between the expression level of APE1 and drug resistance. Accordingly, APE1 has been broadly regarded not only as a quite worthy biomarker for clinical diagnosis but also as a promising tool for screening anticancer drugs and therapeutic targets for cancer [5,6]. Given the significance of APE1, exploiting a subtle and efficient strategy to detect APE1 is of great benefit to clinical practice.

Currently, conventional strategies such as liquid chromatography-mass spectrometry, and enzyme-linked immunosorbent assay (ELISA) have been widely employed to depict the expression levels of APE1 [7]. Fatally, most of these strategies usually were labor-intensive procedures, time-consuming and low abundance, which fall short of meeting the requirements of burgeoning clinical demands. In contrast with the above strategy, the fluorescent probe-based methods have received much

* Corresponding author. Department of Laboratory Medicine, Zhongnan Hospital of Wuhan University, Wuhan University, Wuhan, People's Republic of China.
E-mail address: liyirong838@163.com (Y. Li).
[1] These authors contributed equally to this study.

https://doi.org/10.1016/j.talanta.2025.128161
Received 21 February 2025; Received in revised form 11 April 2025; Accepted 14 April 2025
Available online 15 April 2025
0039-9140/© 2025 Elsevier B.V. All rights are reserved, including those for text and data mining, AI training, and similar technologies.

attention for their simplicity and robustness. For example, Madhusudan et al. established an assay for APE1 activity using fluorophore/quencher-labeled dsDNA substrate and screened for APE1 inhibitors [8]. Zhao et al. developed a label-free strategy for detecting APE1 activity by using ATMND (2-amino-5,6,7-trimethyl-1,8-naphthyridine) as a signal probe [9]. Although these methods mentioned above provide good performance in terms of selectivity and simplicity, their applications are often burdened by limited sensitivity. Therefore, over the last few years, to sensitive detection of the amount of APE1, multiple analytical approaches have been established utilizing isothermal nucleic acid amplification methods such as RCA, CHA, TdT, DNAzyme, and so on [10–18]. Nonetheless, the intricate nature of these components complicates the detection workflow, often necessitating multi-step manual procedures and inevitably reducing both the amplification efficiency and convenience. Thus, it would still be anticipated to develop a simple, sensitive and reliable technique to detect the low-concentration APE1.

The CRISPR system, a prokaryotes adaptive immune defense mechanism, defends the invasion of foreign genes and resists the damage [19,20]. As research on the CRISPR/Cas system advanced, various members of the CRISPR family with distinct characteristics were identified [21], including Cas9 [22–24], Cas12 [25–29], Cas13 [30], and Cas14 [31] paving the way for novel applications in CRISPR molecular biosensing. Among them, Cas12a has been broadly used to detect the target dsDNA containing PAM or ssDNA by crRNA-guided, complementarity-dependent CRISPR recognition, involving both cis and trans cleavage activities, which greatly makes Cas12a/crRNA become a hopeful signal amplifier [32]. For example, Hou et al. effectively harnessed the activity of APE1 to produce multifarious activation parts that initiate the cleavage function of the Cas12a system [33]. Tang et al. depict a straightforward strategy for detecting APE1 based on the REST (releasing extension signal amplification test) method, which leverages dsDNA as an activator to fully enhance the *trans*-cleavage capability of Cas12a [34].

However, these methods still couldn't overcome the compatibility problem of the one-pot assay. Recently, more evidence demonstrates that the activity of Cas12a could be modulated through structural variations of Cas protein or conformational transition within crRNA or the dsDNA/ssDNA molecule. Especially, researchers found that two truncated nucleic acids as substrates also could cause Cas12a's *trans*-cleavage activity [35–37]. We envisage that through the logical structural design of nucleic acid elements, it can be used to activate the Cas12a system more flexibly. Herein, a pivotal element structure-switchable dsDNA promoter with AP site (Dp-A) was established to manipulate the activity of Cas12a for APE1 detection. In this work, the specific inhibitor part of the Dp-A induced spatial steric hindrance in the absence of APE1, leading to the disruption of Cas12a's binding ability, thereby inhibiting Cas12a's cleavaging ability. When APE1 is present, Dp-A is cleaved, generating a split activator (SA) that initiates a synergistic activation reaction of CRISPR/Cas12a by combining with a truncated activator (TA). Leveraging the cascade cleaving mechanism between the enzymatic reaction and the AsCas12a system, the developed method enables the conversion of the target recognition into Cas12a's switchable cleavage event through the use of structure-switchable Dp-A. Moreover, this devised strategy can gratifyingly screen APE1 inhibitors and monitor APE1 in lysates from cell extractions or clinical serum samples with high sensitivity in one step, which spurs further development and application of the CRISPR system.

2. Experimental section

2.1. Materials and reagents

4'_Hydroxypropiophenone and *tert*-butyl hydroperoxide (TBHP) solution were purchased from Macklin Co., Ltd. (Shanghai, China). Lucanthone was purchased from Shanghai Yuanye Bio-Technology Co., Ltd (Shanghai, China). Modified coagulant was obtained from Servicebio Technology Co., Ltd. (Wuhan, Hubei, China). TEMED (N, N, N, N-Tetramethylethylenediamine) and Acryl/Bis 30 % Solution (29:1) were provided by Sangon Biotech Co., Ltd. (Shanghai, China). HPLC-purified DNA (Tables S1–S3) and TE buffer were offered by Sangon Biotech Co., Ltd. (Shanghai, China). Additional materials and reagents are detailed in the "Supplementary Information" file.

2.2. Apparatus

The low-speed centrifuge and Oscillating vortex blender were supplied by DLAB Scientific Co., Ltd. (Beijing, China). Fresco™ 21 Microcentrifuge was equipped by Thermo Fisher Scientific Co., Ltd (Shanghai, China).

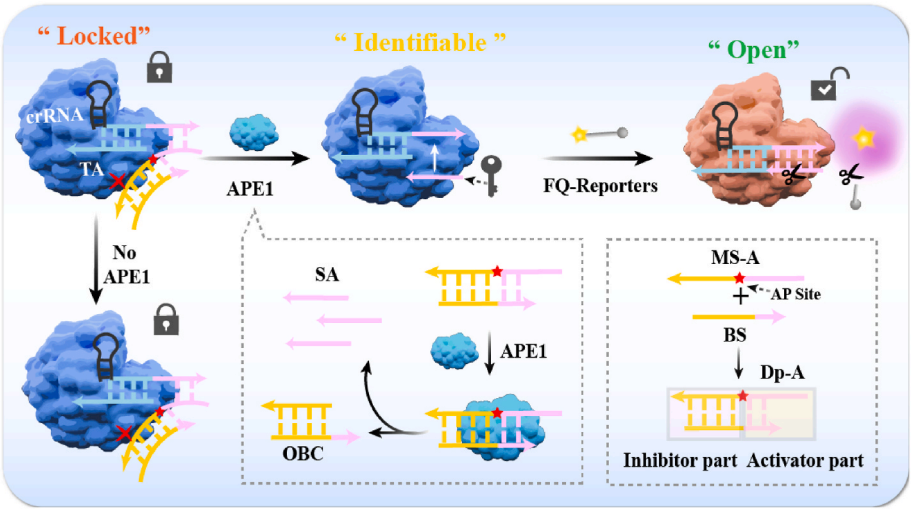
3. Result and discussion

3.1. The design of the APE1-driven structure-switchable -based dsDNA promoter for regulating the cleavage activities of AsCas12a

APE1 exhibits enzymatic activity capable of cleaving the DNA phosphodiester backbone at the 5′ side of an abasic (AP) site in dsDNA, generating a single-strand break with a 3' hydroxyl terminus and a 5' deoxyribose phosphate (dRP) group. Here, by taking full advantage of this feature of APE1, we devised a novel approach EDC that integrates APE1-powered site-directed incision of structure-switchable Dp-A with CRISPR/Cas12a assay to realize sensitive detection of tumor biomarker APE1. The Dp-A contains a modified strand with AP sites (MS-A) and a blocker strand (BS). Moreover, the configurations of Dp-A were divided into two regions with the AP site as the boundary: the inhibitor region creates steric hindrance rendering it non-complementary to crRNA, while the activator region remains complementary to crRNA. When the target APE1 is present, "Dp-A″ serves as an "enzymatic switch element" incising DNA adjacent to the AP sites exchanges its spatial conformation to release the SA which couldn't retain base-paired to its complement at 37 °C. Subsequently, the product SA binds to the TA, resulting in the synergistic activation of Cas12a and restoration of its *trans*-cleavage activity. When the target is absent, the inhibitor segment of Dp-A was positioned to create steric hindrance, which potentially prevented the conformational unlocking of the cas12a catalytic site and thereby suppressing the cutting activity of AsCas12a. Therefore, EDC would be a rapid, specific, and sensitive APE1 sensing platform with wide application potential (Scheme 1).

3.2. Feasibility of the proposed method

As APE1-driven cleavage is a crucial step to initiate follow-up amplification-detection, we first checked whether the introduction of APE1 could contribute to the performance of dsDNA-cleavage. Here, we investigated this reaction by using high-resolution PAGE (polyacrylamide gel electrophoresis). As shown in Fig. 1A, it could be found that the lanes from two to three represented MS-A and BS, respectively. Moreover, the lower band exists in lane 4 indicating the successful formation of Dp-A. As expected, the introduction of APE1 could generate detectable degradation bands compared to that of dsDNA (lane 5). Subsequently, to further confirm the feasibility of EDC, we characterized the follow-up step still by PAGE. When fully activated by the target APE1, the random ssDNA showed a noticeable reduction in intensity in Lane 8 compared to Lane 6. However, no significant changes in random ssDNA were observed when the reaction was conducted in the absence of the target (Lane 7). Taken together, these outcomes reveal that the target-directed cleavage of Dp-A successfully induces AsCas12a's *trans*-cleavage function. Then, the fluorescence spectrum was implemented to substantiate the above results. As seen in Fig. 1B/C, an obvious increase in fluorescence intensity could be observable when APE1 exists compared with no APE1. We further checked the viability of our method



Scheme 1. Schematic diagram of utilizing APE1-activated structure-switchable dsDNA promoter with AP site to trigger the *trans*-cleavage activity of CRISPR/AsCas12a.

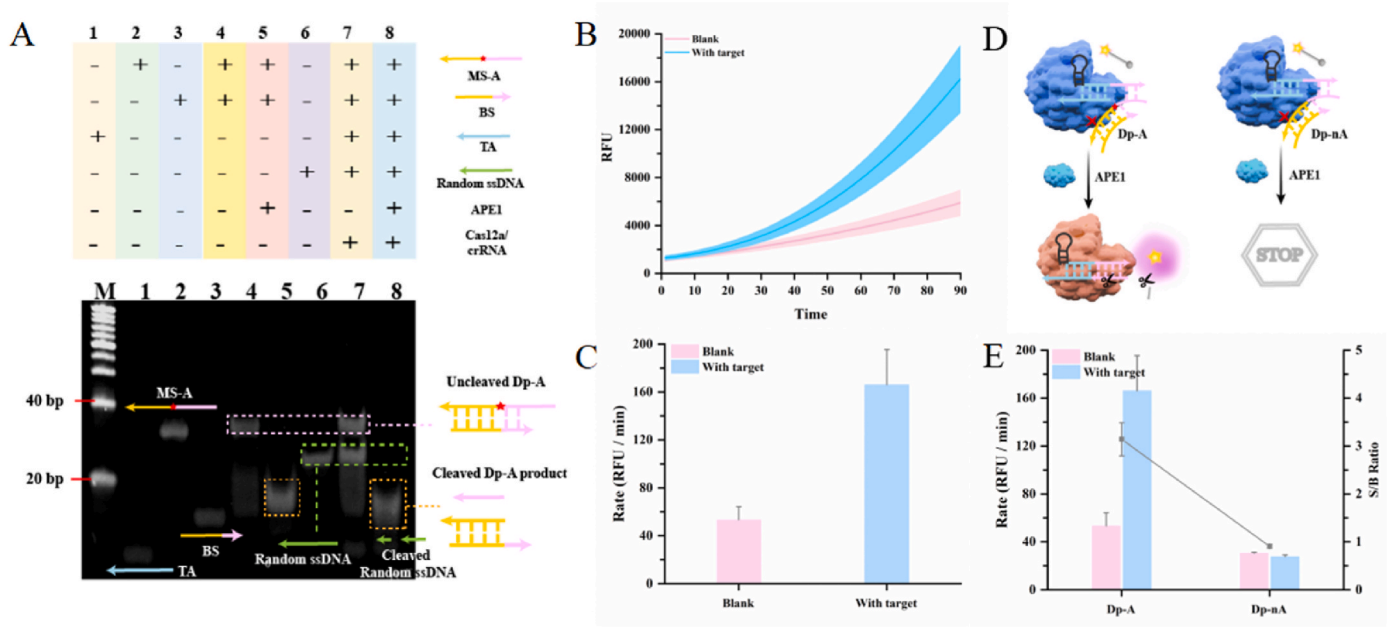


Fig. 1. Feasibility assessment of the proposed strategy. (A) PAGE analysis of the feasibility. Lane 1:TA; Lane 2: MS-A; Lane 3: BS; Lane 4: Dp-A; Lane 5: Dp-A with APE1, Lane6: random ssDNA; Lane 7: the TA/Dp-A complex, AsCas12a/crRNA complex and the random ssDNA; lane 8: the TA/Dp-A complex, APE1 with AsCas12a/crRNA complex and the random ssDNA; (B) The time-dependent fluorescence signals of the EDC initiated method were monitored with and without the target; (C) The fluorescence change rate associated with the reaction shown in Fig. 1B. (D) Schematic illustrating the design of Dp-A, Dp-nA, respectively. (E) The rate of the fluorescence of Dp-A, Dp-nA in response to APE1. Bars represent the mean ± SD (n = 3).

by comparing the fluorescence changes caused by the reactions including different components (Fig. S1). In the absence of MS-A or TA, they can only partially hybridize with the crRNA sequence, failing to activate the AsCas12a and thus preventing the generation of fluorescent signals. Besides, in the absence of BS, there is also shown low fluorescent signal since MS-A chains alone cannot facilitate the cutting of APE1. Simultaneously, minimal fluorescence was detected in the absence of AsCas12a or crRNA. The above results indicate that the incomplete structure did not generate significant fluorescence signals. Therefore, only when the complete structure is present, Dp-A would release detectable SA due to APE 1 cleavage, enabling the formation of proximity ligation DNA module that hybridizes with crRNA, which significantly enhances the activity of AsCas12a.

To further determine whether the AP site plays a key element switch during the whole reaction, we used the dsDNA probe without the AP site (Dp-nA) which has the same structure as Dp-A but lacks AP site as the control. As depicted in Fig. 1D/E and Fig. S2, when the target is absent, neither method was capable of activating AsCas12a, and both yielded negligible background signals owing to the steric hindrance effect. In comparison, the captured S/B (signal-to-background) ratio of the complex with the AP site significantly exceeded that of the complex without the Ap site in the presence of the target, indicating that the AP site was essential for the system.

3.3. *Optimization of the proposed system*

To further investigate the better cleavage efficiency of APE1 and AsCas12a, the number of complementary base pairings of the inhibitor

part of Dp-A which is critical for APE1's enzymatic activity was systematically analyzed. As shown in Fig. 2A, a series of paired Dp-A with different lengths were designed. As depicted in Fig. 2B and Fig. S3, the S/B ratio increased as the number of complementary bases increased until 12 nt due to the too-short length of the strand may result in the dsDNA bond not being stable enough to effectively activate the APE1. Therefore, the 12 nt complementary lengths of the inhibitor region were selected for the detection. Besides, we researched the favorable base length of the activator part of BS (Fig. 2C). As depicted in Fig. 2D and Fig. S4, the S/B ratio enhanced with the growing number of complementary bases until 8 nt then reduced, which can be on account of the too long strand of the activator part of BS might cause incomplete release of SA and reduce its efficiency in activating Cas12a. Therefore, the activator part of BS with 8 nt complementary lengths was chosen for subsequent experiments.

To further investigate the detection efficiency of the target, additional essential experimental conditions including the concentration of the AsCas12a/crRNA complex and the Dp-A/TA complex, and the ratio of AsCas12a/crRNA complex were optimized. As depicted in Fig. 2E and Fig. S5, the concentration of the Dp-A/TA was detected from 200 to 1 nM. The S/B ratio improved as the concentrations of Dp-A/TA increased from 200 to 100 nM. Then, the S/B ratio exhibited a gradual decline which can be attributed to that too little or too high Dp-A/TA might suppress the cut reaction. Subsequently, to balance the reaction and background signal, 100 nM was taken for further investigations. As depicted in Fig. 2F and Fig. S6, the S/B ratio increased as the ratio of the Cas12a/crRNA complex rose, reaching its peak at a 1:1 ratio. Therefore, the 1:1 proportion was chosen in the following experiments. Next, further optimization was performed on the concentration of the Cas12a/crRNA complex (Fig. 2G and Fig. S7). The concentration progressively increased and attained a peak value at 100 nM. A significant decrease will be observed if the concentration of Cas12a/crRNA falls below 100 nM. Thus, 100 nM was chosen as the optimum concentration.

3.4. Evaluation of the analytical performance and application of this strategy

Using the optimized conditions, we further investigated the analytical performance by measuring the detection sensitivity at different target concentrations. As shown in Fig. 3A, the fluorescence enhanced as the concentration of APE1 increased from 5.0×10^{-5} to 1.0 U/mL. Besides, the calibration plots of APE1 were depicted in the inset of Fig. 3B. The linear formula is $Y = 128266.03\ C_{target} + 1071.40$ ranging from 5.0×10^{-5} to 1.0×10^{-1} U/mL with the LOD calculated to be 4.8×10^{-5} U/mL. The proposed strategy effectively distinguished fluorescence intensities across varying concentrations, demonstrating the capability of this strategy would provide a clear response to different target concentrations. Besides, compared to other reported CRISPR/Cas12a-based APE1 detection methods (Table S4), which require sophisticated multi-step manual operations based on the usage of nanomaterials or enzymes for signal transduction or amplification, our sensing system could react in one pot, achieving a low detection limit within a relatively short time. This approach improves the stability of the detection assay and reduces the cost significantly. Besides, since the considerable amplification efficiency of APE1 and the extraordinary performance of Cas12a, the proposed biosensor presented great potential for APE1 detection applications.

We further validated the selectivity of the proposed method using various proteins including restriction endonucleases (*Dpn*I), Structure-specific Endonucleases (UDG, FEN1), Exonucleases and Non-specific Endonucleases Products (Lambda Exonuclease) and Restriction Endonucleases (Nt.*Bbv*CI). Fig. 3C and D illustrate the fluorescence intensities for different targets. Significant differences were observed between the fluorescence signals of non-specific groups and those from APE1 detection. Moreover, a mixture of APE 1 together with the same concentration of other interfering enzymes was detected and the fluorescence signal was almost the same as the fluorescence signal caused by only APE1. Accordingly, the sensor demonstrated superior performance

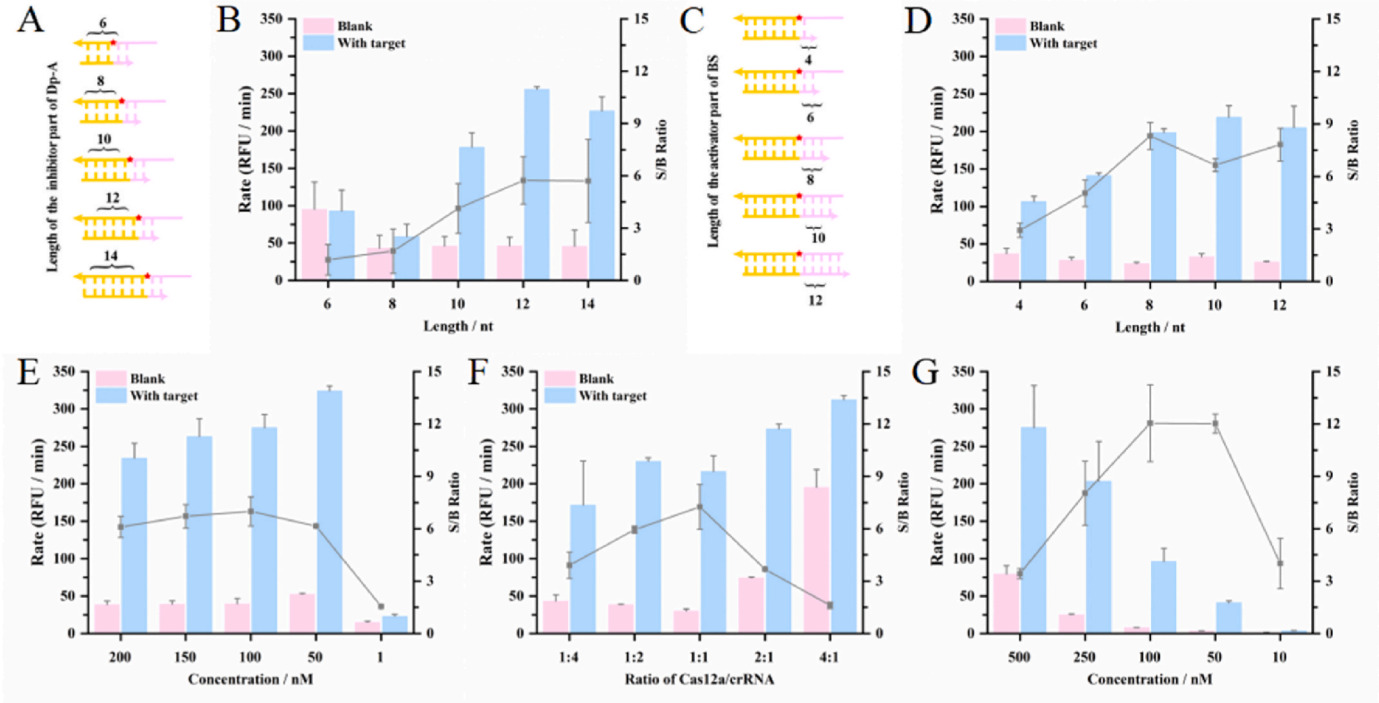


Fig. 2. To detect the optimal conditions for this experiment. (A) Schematic illustration of the inhibitor part of Dp-A with different lengths; (B) The fluorescence rates and S/B ratios produced by the inhibitor part of Dp-A with different lengths; (C) Schematic illustration of the activator part of BS with different lengths; (D) The fluorescence rates and S/B ratios produced by the activator part of BS with different lengths; (E) The fluorescence rates and S/B ratios produced by different concentration of Dp-A/TA; (F) The fluorescence rates and S/B ratios produced by the different ratio of Cas12a/crRNA; (G) The fluorescence rates and S/B ratios produced by the different concentration of Cas12a/crRNA. Bars represent the mean ± SD (n = 3).

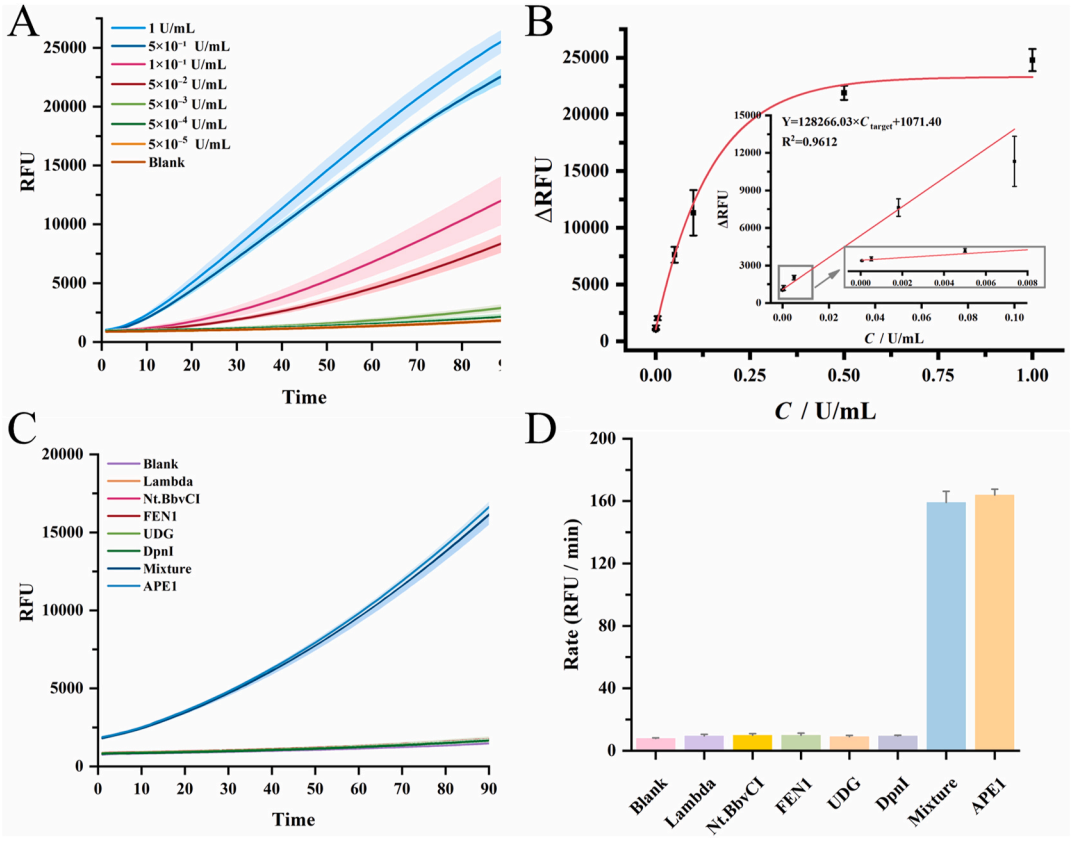


Fig. 3. Analytical performance of this strategy. (A) Time-dependent fluorescence signals with different concentrations of APE1 from 5.0 × 10^{-5} to 1.0 U/mL. (B) Fluorescence intensity was responding to the reaction in Fig. 3A. The linear correlation of the devised method of fluorescence intensities for different amounts of APE1 was shown in the inset. (C) Time-dependent fluorescence signals are produced by various proteins; (D) The rate of the fluorescence of other proteins and APE1. Bars represent the mean ± SD (n = 3).

in discriminating APE1 from other types of proteins, highlighting its strong potential for selective and efficient target detection.

3.5. Application assessment of the devised strategy

Currently, it has been discovered that suppression of the APE1's activity can impede cancer progression, making it a promising target for the development of anticancer drugs. To assess the utility of the proposed strategy for inhibitor screening, NCA, 4'_Hydroxypropiophenone and Lucanthone, well-established and selective APE1 inhibitors that effectively inhibit APE1's AP endonuclease activity, were chosen as the positive control. Besides, TBHP was chosen as the negative control. As seen in Fig. 4A and Fig. S8A, the stronger fluorescence was discovered in the negative conditions. In contrast, the fluorescence was weak in the positive group indicating that NCA, 4'_Hydroxypropiophenone and Lucanthone would be expected to block the APE1 cleavage-induced recognition and thus block the entire reaction. Under the same conditions, the relative activity of APE1 was concentration-dependent in the range of 80–800 μM NCA (Fig. 4B), and the IC50 value was determined to be 420.3 μM (Fig. 4C). The above result demonstrates that this system could be effectively utilized for screening APE1 inhibitors.

To investigate the broad application prospects of the suggested method in complex biological samples, a cell lysis test was performed. Initially, to exclude the influence of RIPA lysate on the experiment, different concentrations of target APE1 were added to DEPC and RIPA buffers for fluorescence detection. As seen in Fig. S9, it shows the fluorescence intensity of target APE1 with different concentrations was nearly identical in both DEPC and RIPA buffers. Then, the expression level of APE1 protein derived from cell lysates, containing HEK-293 T, A549, MDA/MB-231 and Huh7, was detected with or without the addition of the inhibitor. As seen in Fig. 4D and Fig. S10A, these results indicated that the fluorescence signals were rapidly decreased after adding the NCA, further evidence of NCA specifically inhibits the endogenous APE1 activity response is provided. Next, analysis of A549 cell lysates with different cell numbers showed a gradual decrease in fluorescence intensity as the number of A549 cells decreased (Fig. 4E and Fig. S10B). Besides, the calibration plots of Fig. 4F show an "S" relationship between the fluorescent intensities and the logarithm of A549 concentration which is from 10 to 10,000 cells/mL. The above results indicate that this strategy can precisely quantify the activity of intracellular APE1, showcasing significant potential for clinical diagnosis.

3.6. Detection of APE1 activity from biological samples

Motivated by the outstanding detection capabilities of EDC, we were prompted to explore the APE1 activity of biological samples. To evaluate whether APE1 expression levels are elevated in lung cancer, we collected serum samples from 30 patients with histopathologically confirmed diagnoses as the case group. A total of 30 healthy individuals, with no history of tumors or other diseases, were recruited from the health examination center at our hospital. Then, we used a commercial ELISA kit and EDC for APE1 detection. As depicted in Fig. 5A/B and Fig. S11/12, the expression level of APE1 in the serum of patients was higher than that in the serum of healthy controls. The area under the ROC curve (AUC) value of EDC was 0.8578. Through optimization of the cut-off value to maximize the combined sensitivity and specificity, we achieved an optimal balance with 83.33 % sensitivity and 96.67 % specificity (Fig. 5C). Additionally, the samples were analyzed using ELISA for method comparison (Fig. 5D–F). The above results showed

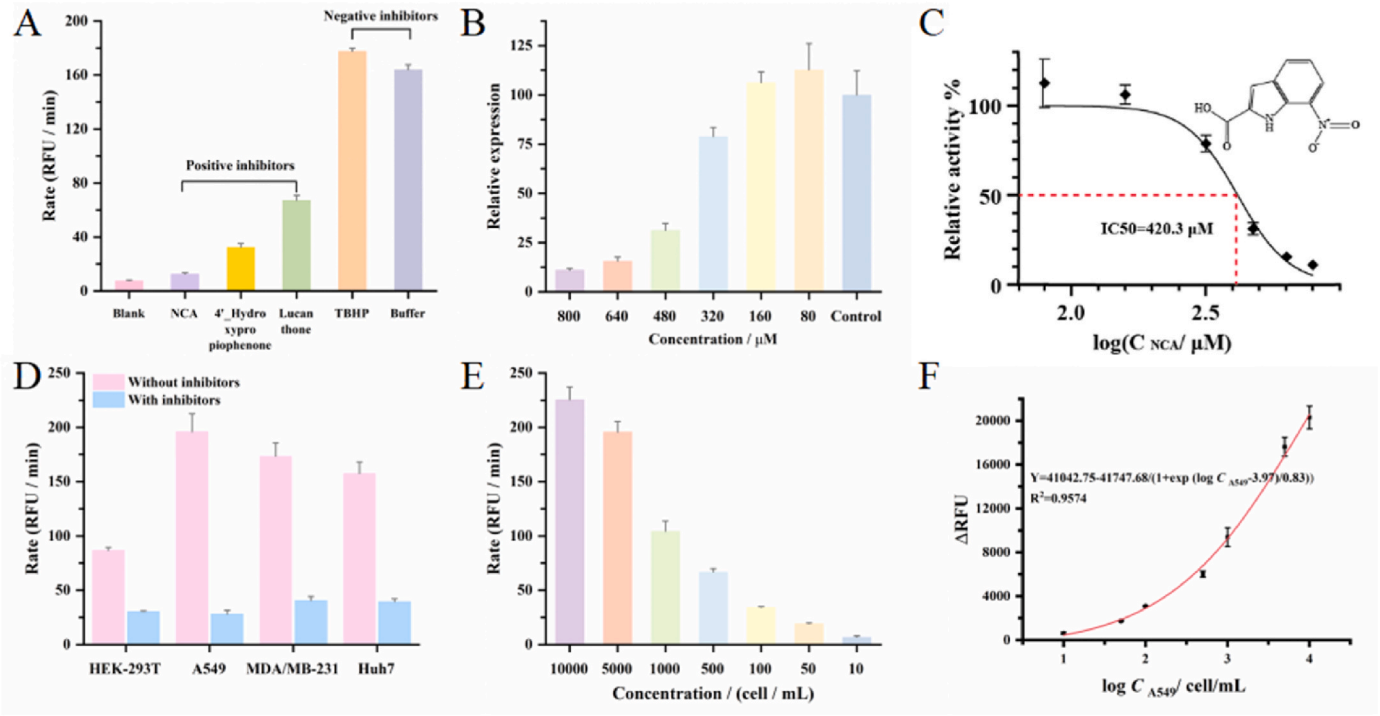


Fig. 4. Application of this devised method. (A) Evaluation of the inhibitory effects of various chemical substances on APE1; (B) Detection of the relative fluorescence expression triggered by different concentrations of APE1 inhibitor. (C) The inhibitory effect evaluation of various concentrations of APE1 inhibitor (NCA) on APE1. (D) The fluorescence rates were examined in different cancer cell lysates with or without inhibitors. (E) Analysis of the expression of APE1 in A549 cell lysates at different concentrations (10–10000 cells/mL). (F) Curve relationship between the fluorescence intensity and the logarithm of A549 cell. Bars represent the mean ± SD (n = 3).

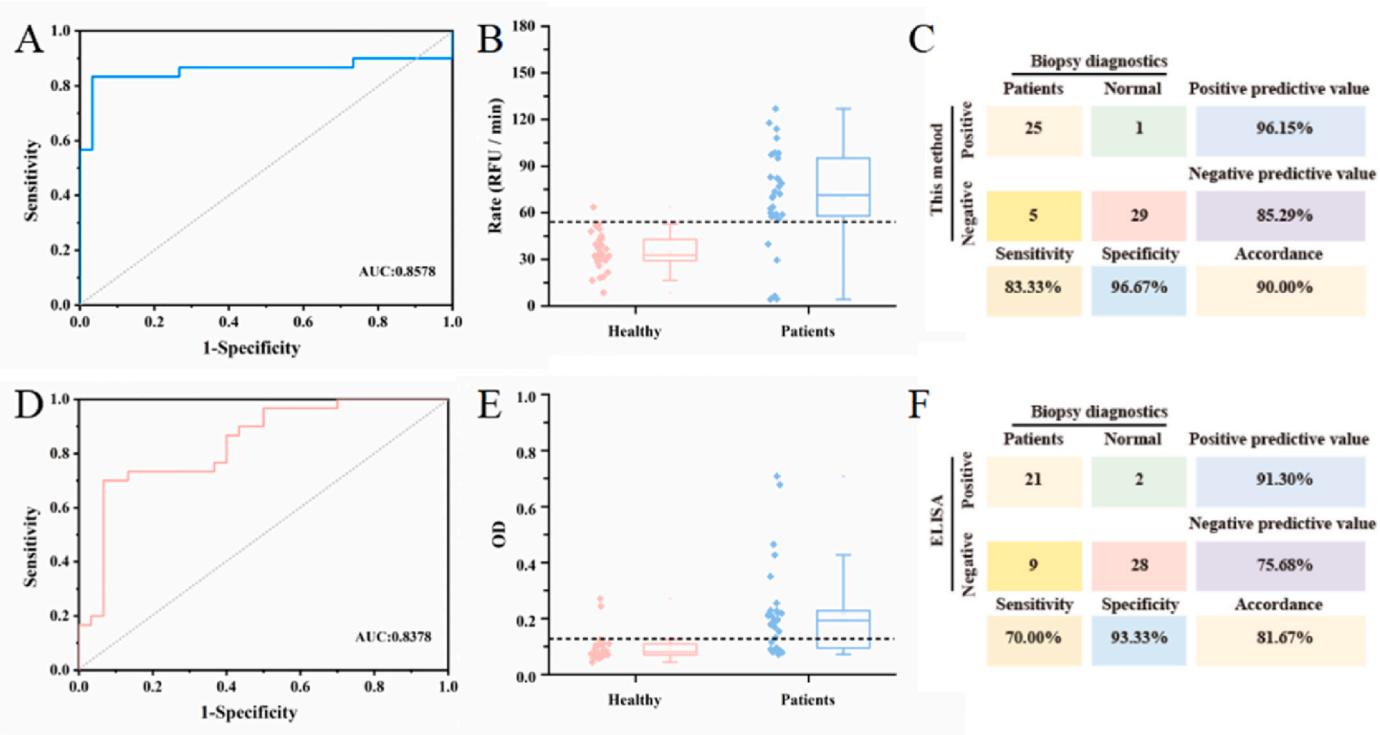


Fig. 5. Analysis of APE1 enzyme activity in clinical samples. (A) The ROC curves of clinical serum samples diagnostic model using EDC methods. (B) Box plot for detection of activity of APE1 by using EDC methods. (C) Performance of proposed EDC compared to biopsy diagnostics (gold standard). (D) The ROC curves of clinical serum samples diagnostic model using ELISA methods. (E) Box plot for detection of activity of APE1 by using ELISA method. (F) Performance of commercial ELISA kit compared to biopsy diagnostics (gold standard). (For interpretation of the references to colour in this figure legend, the reader is referred to the Web version of this article.)

that this devised method based on EDC was consistent with those of standard ELISA, indicating that our devised sensor can detect APE1 which is higher sensitivity and more convenient than traditional ELISA methods.

4. Conclusion

This study introduces a novel approach by developing a programmable construction-adjustable promoter to control the activity of Cas12a. By utilizing target-triggered site-directed cleavage, this strategy effectively mitigates steric hindrance, enabling the activation of AsCas12a and allowing for real-time, user-friendly and portable APE1 detection. Furthermore, by harnessing the robust enzymatic and catalytic cleavage of CRISPR, this strategy achieves faster detection of APE1 at a constant physiological temperature, offering distinct advantages over traditional techniques. Most importantly, the entire detection process can be performed in a single pot, significantly minimizing the need for specific external environmental conditions and greatly simplifying the experimental procedure. In conclusion, this study offers novel perspectives on modulating Cas12a's *trans*-cleavage activity through steric hindrance-based inhibitors, presenting a promising sensing platform for protein detection in molecular diagnostics.

CRediT authorship contribution statement

Xingrong Li: Writing – original draft, Project administration, Methodology, Investigation. **Yumei Li:** Resources, Formal analysis, Data curation. **Cuixiang Wang:** Validation, Software, Investigation. **Jiatong Chai:** Methodology, Formal analysis. **Hongmao Liu:** Data curation, Conceptualization. **Xinli Jiang:** Validation, Resources. **Yirong Li:** Writing – review & editing, Supervision, Project administration, Funding acquisition, Data curation.

Declaration of competing interest

The authors declare that they have no known competing financial interests or personal relationships that could have appeared to influence the work reported in this paper.

Acknowledgments

This research was funded by financial support from the Key R & D Projects of Hubei Province(2022BCA019) and the Hubei Provincial Public Leadership Talents Project(WSJKRC2025007).

Appendix A. Supplementary data

Supplementary data to this article can be found online at https://doi.org/10.1016/j.talanta.2025.128161.

Data availability

Data will be made available on request.

References

[1] T.M. Weaver, N.M. Hoitsma, J.J. Spencer, L. Gakhar, N.J. Schnicker, B. D. Freudenthal, Structural basis for APE1 processing DNA damage in the nucleosome, Nat. Commun. 13 (2022) 5390.
[2] L. Li, N. Li, S. Fu, Y. Deng, C. Yu, X. Su, Base excision repair-inspired DNA motor powered by intracellular apurinic/apyrimidinic endonuclease, Nanoscale 11 (2019) 1343–1350.
[3] A.M. Whitaker, B.D. Freudenthal, APE1: a skilled nucleic acid surgeon, DNA Repair 71 (2018) 93–100.
[4] T.C. Liu, K.W. Guo, J.W. Chu, Y.Y. Hsiao, Understanding APE1 cellular functions by the structural preference of exonuclease activities, Comput. Struct. Biotechnol. J. 19 (2021) 3682–3691.
[5] S. Choi, J.H. Shin, Y.R. Lee, H.K. Joo, K.H. Song, Y.G. Na, S.J. Chang, J.S. Lim, B. H. Jeon, Urinary APE1/Ref-1: a potential bladder cancer biomarker, Dis. Markers 2016 (2016) 7276502.
[6] S. Thakur, B. Sarkar, R.P. Cholia, N. Gautam, M. Dhiman, A.K. Mantha, APE1/Ref-1 as an emerging therapeutic target for various human diseases: phytochemical modulation of its functions, Exp. Mol. Med. 46 (2014) e106.
[7] N. Dai, X.-J. Cao, M.-X. Li, Y. Qing, L. Liao, X.-F. Lu, S.-H. Zhang, Z. Li, Y.-X. Yang, D. Wang, Serum APE1 autoantibodies: a novel potential tumor marker and predictor of chemotherapeutic efficacy in non-small cell lung cancer, PLoS One 8 (2013) e58001.
[8] S. Madhusudan, F. Smart, P. Shrimpton, J.L. Parsons, L. Gardiner, S. Houlbrook, D. C. Talbot, T. Hammonds, P.A. Freemont, M.J.E. Sternberg, G.L. Dianov, I. D. Hickson, Isolation of a small molecule inhibitor of DNA base excision repair, Nucleic Acids Res. 33 (2005) 4711–4724.
[9] X. Li, M. Xiong, Y. Huang, L. Zhang, S. Zhao, Simple label-free fluorescence detection of apurinic/apyrimidinic endonuclease 1 activity and its inhibitor using the abasic site-binding fluorophore, Anal. Methods 11 (2019) 739–743.
[10] M. Chen, Y. Xia, Z. Qiu, S. Zhu, Y. Wang, X. Luo, Enzymes-mediated facile biosynthesis of G-quadruplexes for sensitive detection of apurinic/apyrimidinic endonuclease 1 activity, Microchem. J. 196 (2024) 109579.
[11] Y. Hu, Z. Zhang, W. Ye, W. Zhang, M. Hu, W. Yuan, et al., A DNA structure-mediated fluorescent biosensor for apurinic/apyrimidinic endonuclease 1 activity detection with ultra-high sensitivity and selectivity, Sensor. Actuator. B Chem. 330 (2021) 129332.
[12] C. Li, Y. Hu, T. Shi, K. Dong, T. Wu, Label-free colorimetric detection platform based on catalytic hairpin self-assembly and G-quadruplex/hemin DNAzyme for comprehensive biomarker profiling, Talanta 272 (2024) 125835.
[13] J. Meng, Z. Xu, X. Li, B. Wang, X. Zhang, Z. Xie, C. Zhang, H. Wang, Y. Zhang, Synergistic powering of DNA walker movement by endogenous dual enzymes for constructing dual-mode biosensors, Biosens. Bioelectron. 262 (2024) 116566.
[14] X. Wang, J. Meng, H. Zhang, J. Mou, J. Xiong, H. Wang, X. Su, Y. Zhang, Electrochemical biosensor based on bipedal DNA walker for highly sensitive amplification detection of apurinic/apyrimidinic endonuclease 1, Sensor. Actuator. B Chem. 381 (2023) 133425.
[15] C. Xu, S. Chen, J. Zhao, X. Luo, S. Zhao, A DNAzyme-mediated target-initiated rolling circle amplification strategy based on a microchip platform for the detection of apurinic/apyrimidinic endonuclease 1 at the single-cell level, Chem. Commun. 57 (2021) 11017–11020.
[16] L.-R. Hong, W. Li, M.-Y. Lu, H. Xu, W. Liu, Y. Zhu, Y. Zhuo, Simplified rolling circle amplification driven in situ generation of electrochemiluminescent silver nanoclusters for APE1 activity monitoring, Sensor. Actuator. B Chem. 397 (2023) 134699.
[17] Y. Yang, N. Zhang, W. Jiang, Acid-responsive mediated entropy driven signal amplification nanosystem for sensitive imaging of APE1 activity in living cells, Sensor. Actuator. B Chem. 399 (2024) 134858.
[18] S. Zeng, J. Chen, C. Qi, Y. Shang, Y. Yang, J. Chen, Ligation initiated self-priming isothermal polymerization enabled nano-signal amplification for APE1 sensing and logical unlocking, Sensor. Actuator. B Chem. 420 (2024) 136467.
[19] R. Barrangou, CRISPR-cas systems and RNA-Guided interference, Wiley Interdiscip Rev RNA 4 (2013) 267–278.
[20] S. Shmakov, A. Smargon, D. Scott, D. Cox, N. Pyzocha, W. Yan, O.O. Abudayyeh, J. S. Gootenberg, K.S. Makarova, Y.I. Wolf, K. Severinov, F. Zhang, E.V. Koonin, Diversity and evolution of class 2 CRISPR-cas systems, Nat. Rev. Microbiol. 15 (2017) 169–182.
[21] K.S. Makarova, F. Zhang, E.V. Koonin, SnapShot: class 2 CRISPR-cas systems, Cell 168 (2017) 328–328.e1.
[22] C. Anders, O. Niewoehner, M. Jinek, In vitro reconstitution and crystallization of Cas9 endonuclease bound to a guide RNA and a DNA target, Methods Enzymol. 558 (2015) 515–537.
[23] F. Jiang, J.A. Doudna, CRISPR-Cas9 structures and mechanisms, Annu. Rev. Biophys. 46 (2017) 505–529.
[24] A.T. Raper, A.A. Stephenson, Z. Suo, Sharpening the scissors: mechanistic details of CRISPR/Cas9 improve functional understanding and inspire future research, J. Am. Chem. Soc. 140 (2018) 11142–11152.
[25] D. Dong, K. Ren, X. Qiu, J. Zheng, M. Guo, X. Guan, H. Liu, N. Li, B. Zhang, D. Yang, C. Ma, S. Wang, D. Wu, Y. Ma, S. Fan, J. Wang, N. Gao, Z. Huang, The crystal structure of Cpf1 in complex with CRISPR RNA, Nature 532 (2016) 522–526.
[26] T. Karvelis, G. Bigelyte, J.K. Young, Z. Hou, R. Zedaveinyte, K. Budre, et al., PAM recognition by miniature CRISPR-Cas12f nucleases triggers programmable double-stranded DNA target cleavage, Nucleic Acids Res. 48 (2020) 5016–5023.
[27] S.Y. Li, Q.X. Cheng, J.K. Liu, X.Q. Nie, G.P. Zhao, J. Wang, CRISPR-Cas12a has both cis- and trans-cleavage activities on single-stranded DNA, Cell Res. 28 (2018) 491–493.
[28] S. Stella, P. Alcon, G. Montoya, Structure of the Cpf1 endonuclease R-loop complex after target DNA cleavage, Nature 546 (2017) 559–563.
[29] D.C. Swarts, M. Jinek, Mechanistic insights into the cis- and trans-Acting DNase activities of Cas12a, Mol. Cell 73 (2019) 589–600.e4.
[30] O.O. Abudayyeh, J.S. Gootenberg, S. Konermann, J. Joung, I.M. Slaymaker, D. B. Cox, S. Shmakov, K.S. Makarova, E. Semenova, L. Minakhin, K. Severinov, A. Regev, E.S. Lander, E.V. Koonin, F. Zhang, C2c2 is a single-component programmable RNA-guided RNA-Targeting CRISPR effector, Science 353 (2016) aaf5573.
[31] L.B. Harrington, D. Burstein, J.S. Chen, D. Paez-Espino, E. Ma, I.P. Witte, J. C. Cofsky, N.C. Kyrpides, J.F. Banfield, J.A. Doudna, Programmed DNA destruction by miniature CRISPR-Cas14 enzymes, Science 362 (2018) 839–842.

[32] L. Zhang, S. Luo, R. Fan, R. Li, W. Li, S. Chen, F. Lan, Y. Zhu, T. Ji, Y. Zhang, L. Li, Localized Cas12a-based cascade amplification for sensitive and robust detection of APE1, Talanta 280 (2024) 126773.
[33] X. Chen, G. Cao, J. Zhang, Y. Deng, X. Luo, M. Yang, D. Huo, C. Hou, An ultrasensitive and point-of-care strategy for enzymes activity detection based on enzyme extends activators to unlock the ssDNase activity of CRISPR/Cas12a (EdU-CRISPR/Cas12a), Sensor. Actuator. B Chem. 333 (2021) 129553.
[34] S. Ding, Y. Yuan, J. Dong, F. Du, X. Cui, Z. Shi, Z. Tang, Leveraging CRISPR/Cas12 signal amplifier to sensitive detection of apurinic/apyrimidinic endonuclease 1 and high-throughput inhibitor screening, Anal. Chim. Acta 1291 (2024) 342212.
[35] Q. Li, Z.-L. Song, Y. Zhang, L. Zhu, Q. Yang, X. Liu, X. Sun, X. Chen, R. Kong, G.-C. Fan, X. Luo, Synergistic incorporation of two ssDNA activators enhances the trans-cleavage of CRISPR/Cas12a, Anal. Chem. 95 (2023) 8879–8888.
[36] S.R. Rananaware, E.K. Vesco, G.M. Shoemaker, S.S. Anekar, L.S.W. Sandoval, K. S. Meister, N.C. Macaluso, L.T. Nguyen, P.K. Jain, Programmable RNA detection with CRISPR-Cas12a, Nat. Commun. 14 (2023) 5409.
[37] X. Li, D. Zhang, X. Cai, X. Shu, Z. Zeng, S. Ding, Y. Yan, Branched DNA switchable CRISPR-Cas12a system for sensing FEN1 activity, Chem. Eng. J. 470 (2023) 144407.